Supplementary Information

Spin-decoupled Excitation and Wavefronts Shaping of Structured Surface Waves *via* On-Chip Terahertz Metasurfaces

Ming-Zhe Chong[1], Yidan He[2], Jin Zhao[1], Yue-Yi Zhang[1], Zong-Kun Zhang[1], Chong-Qi Zhang[1], Chao-Hai Du[1], Xiaofei Zang[3,], and Pu-Kun Liu[1,*]*

[1]State Key Laboratory of Advanced Optical Communication Systems and Networks, School of Electronics, Peking University, Beijing, 100871, China

[2]Key Laboratory for the Physics and Chemistry of Nanodevices, School of Electronics, Peking University, Beijing, 100871, China

[3]Terahertz Technology Innovation Research Institute, and Shanghai Key Lab of Modern Optical System, University of Shanghai for Science and Technology, No. 516 JunGong Road, Shanghai, 200093, China

*Correspondence to *Xiaofei Zang*: xfzang@usst.edu.cn, and *Pu-Kun Liu*: pkliu@pku.edu.cn

A. Simulated cross-polarization reflection coefficients for circularly polarized incidence at 0.24 THz

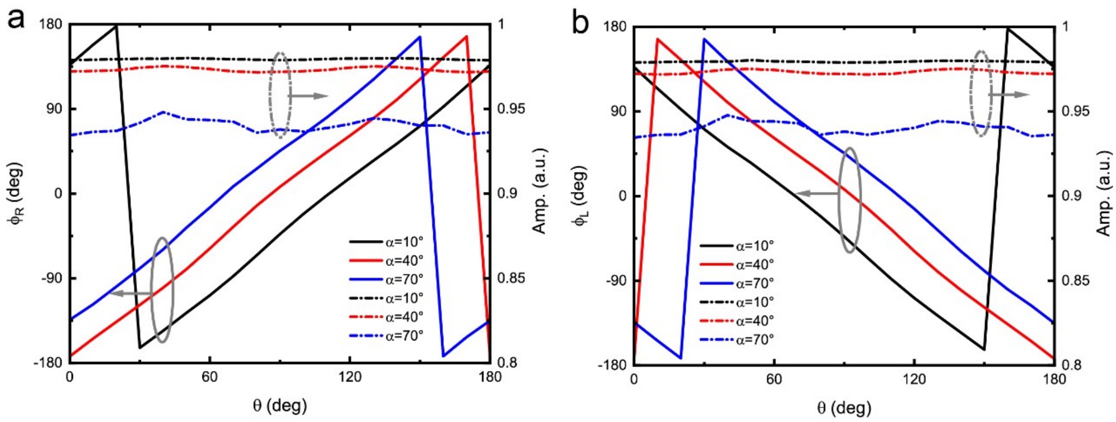

Fig. S1 (a, b) Simulated cross-polarization reflection amplitudes and phases when the incident wave is (a) right circularly polarized (RCP) and (b) left circularly polarized (LCP) with different rotation angles (θ) and opening angles (α) at 0.24 THz.

B. Details about the fabricated meta-device

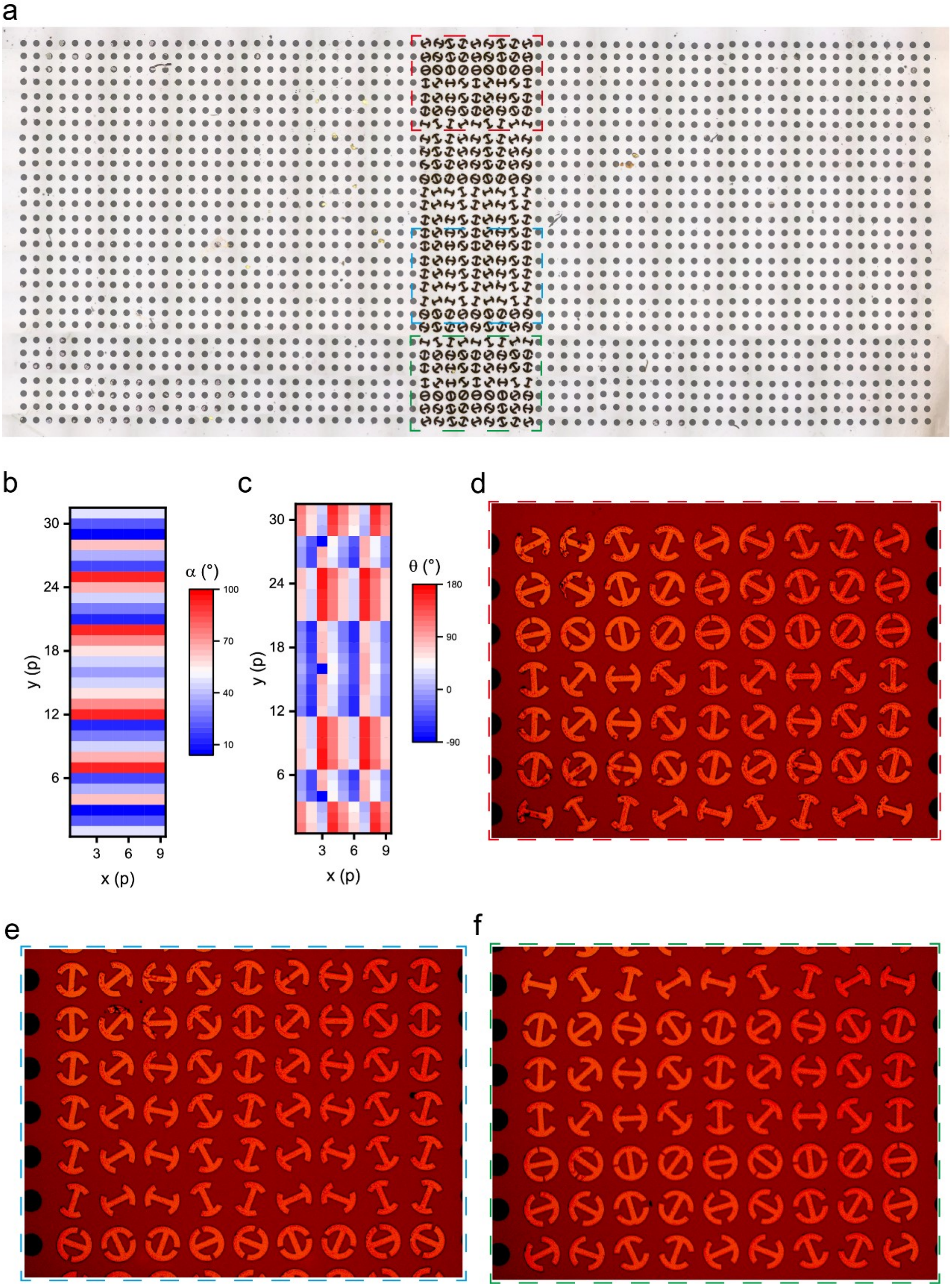

Fig. S2 (a) Optical image of part of the fabricated meta-device (top view). (b) Open angles (α) of all the meta-atoms. (c) Rotation angles (θ) of all the meta-atoms. (d-f) optical images of some meta-atoms (in (d) red, (e) blue, and (f) green boxes of Fig. S2 (a), top view).

C. Details about simulated field distributions of $|E_z|^2$ at 0.24 THz

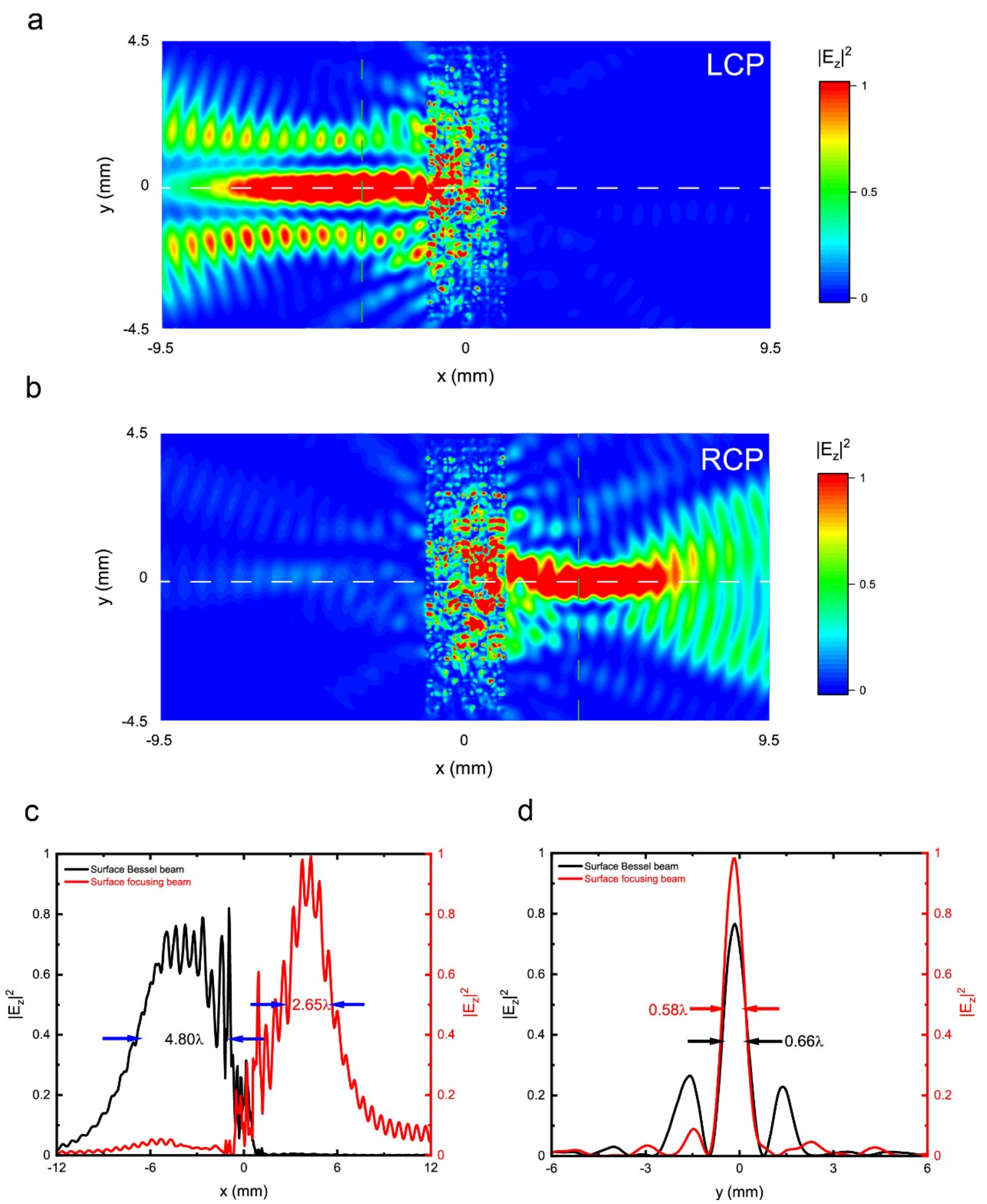

Fig. S3 (a, b) Simulated field distributions of $|E_z|^2$ under (a) LCP and (b) RCP incidence on a plane 50 μm above the device at 0.24 THz. (c) Simulated field distributions of $|E_z|^2$ at white lines (marked in Fig. S3 (a, b), with y = -100 μm). The full width half maximum (FWHM) of the depth of focus (DoF) of SBB and SFB is 4.80λ and 2.65λ, respectively. Ripples and sharp peaks of the curves can be attributed to two factors: 1) Local field enhancement from the resonance of the meta-atoms; 2) Standing wave effect from the impedance mismatch of the side interface between quartz substrate and air. (d) Simulated field distributions of $|E_z|^2$ at green lines (marked in Fig. S3 (a, b), with (a) x =

-3,800 μm, and (b) x = 3,800 μm). The full width half maximum (FWHM) of the spot size of SBB and SFB is 0.66λ and 0.58λ, respectively.

D. Working efficiency of the designed meta-device

Working efficiency is depicted in Fig. S4 to quantitatively characterize the performance of the designed meta-device. The working efficiency is defined as the ratio between the power carried by SBB or SFB that flows on the device in the desired area and the total effective incident power. In this scenario, the working efficiency is:

$$\eta = \left| \frac{\iint_{\Sigma_{out}} S_x dydz}{\iint_{\Sigma_{in}} S_z dxdy} \right| \qquad \text{(S1)}$$

where $S_{x,z}$ is the x or z component of the Poynting vector, Σ_{in} is the integral area of the effective incident beam (with z = 100 μm, x ranging from -1,250 μm to 1,250 μm, y ranging from -4,300 μm to 4,300 μm, black dashed boxes in Fig. S4 (a, b)), and Σ_{out} is the integral area of SBB or SFB in certain places (with x = -3,800 μm (for SBB) or x = 3,800 μm (for SFB), y ranging from -900 μm to 700 μm (slight deviation from the center), z ranging from -300 μm to 1,550 μm, red line in Fig. S4 (a), and blue line in Fig. S4 (b), top view). The effective incident power (in black dashed boxes, Fig. S4 (a, b)), and the power flowing along the x-direction in desired areas (red line in Fig. S4 (a), and blue line in Fig. S4 (b), top view) are integrated to calculate efficiency. After calculation, the working efficiencies of both SBB and SFB are depicted in Fig. S4 (c). The simulated working efficiencies of SBB and SFB at 0.24 THz are 55% and 76%, respectively. It is worth noting that the working efficiency of SBB is lower than that of SFB since the side lobes of SBB carry part of the power, which is not in the integral area. Regretfully, we cannot obtain the working efficiency of the device in the experiment because of the limitation of the experimental equipment. In the future, we hope to improve our equipment to obtain the efficiency of the designed device in the experiment.

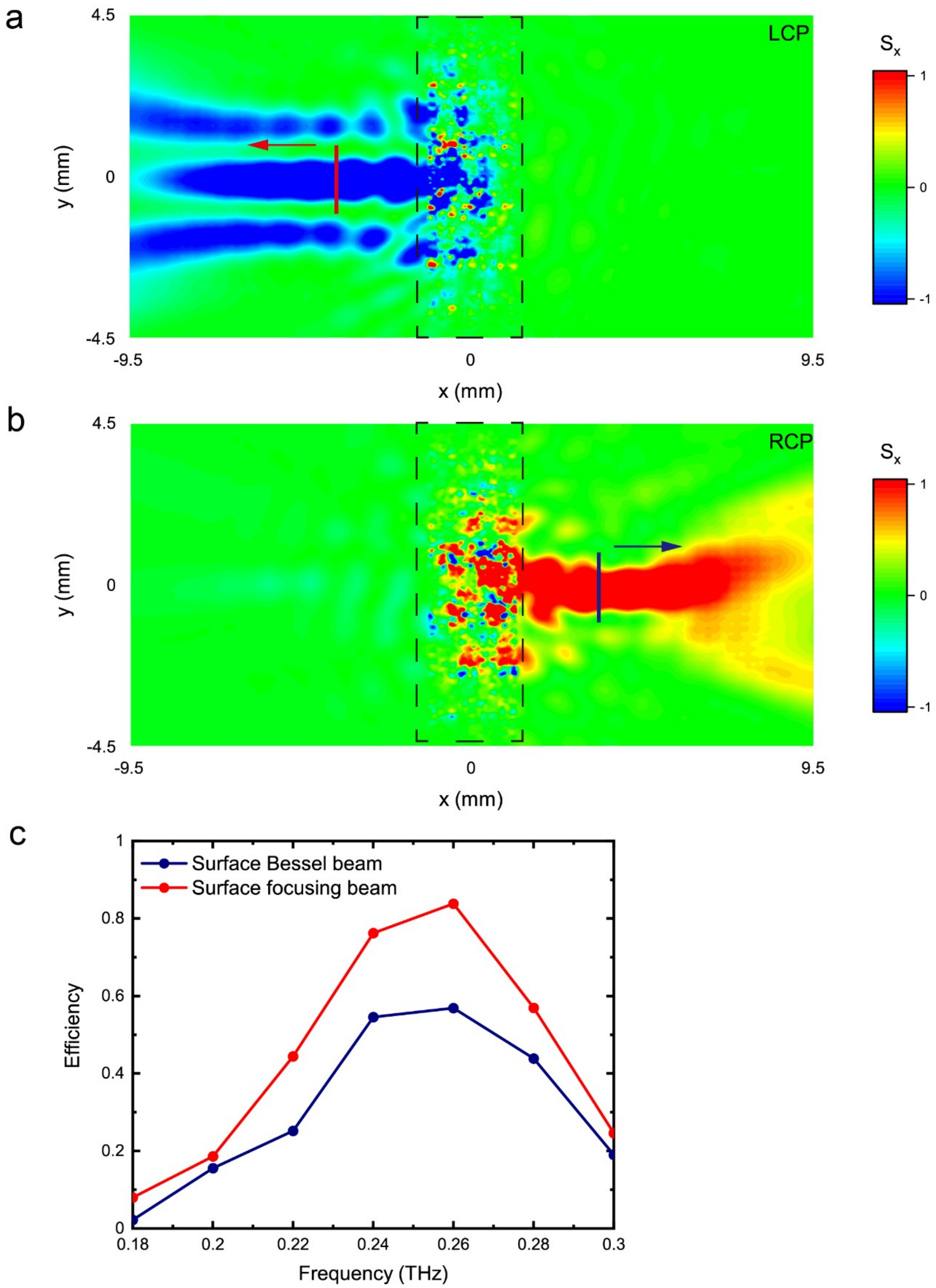

Fig. S4 (a, b) Simulated power flow distributions of S_x under (a) LCP and (b) RCP incidence on a plane 50 μm above the device at 0.24 THz. (c) Simulated working efficiency of SBB and SFB at different frequencies.

E. Simulated field distributions under LP incidence at different frequencies.

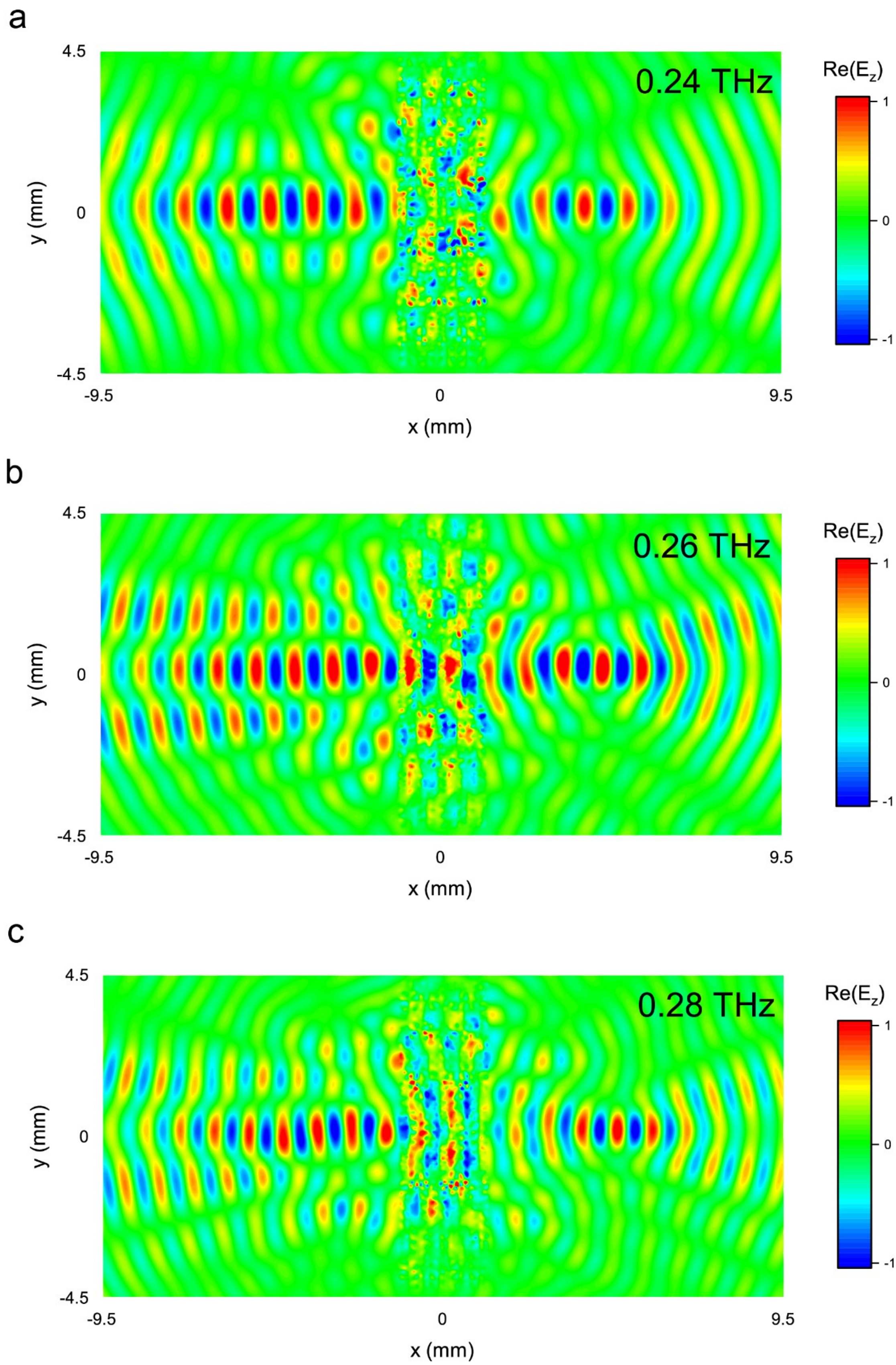

Fig. S5 (a-c) Simulated field distributions of Re(E_z) under *x*-pol incidence on a plane 50 μm above the device at (a) 0.24 THz, (b) 0.26 THz, and (c) 0.28 THz. The SBB is formed on the left side of the meta-device, while the SFB is formed on the right side.

F. Relationship of resonance phase between surface waves and propagating waves

In order to estimate the linear factor between the resonant phase for surface waves and that for propagating waves, we perform full-wave simulations to study the influences brought by different linear factors, as depicted in Fig. S6. Through observing the simulated results of different meta-devices composed of meta-atoms with different linear factors (1.00, 1.18, and 1.39), we think the factor of 1.39 may be better. Nonetheless, other factors may also be accepted if in an adequate range.

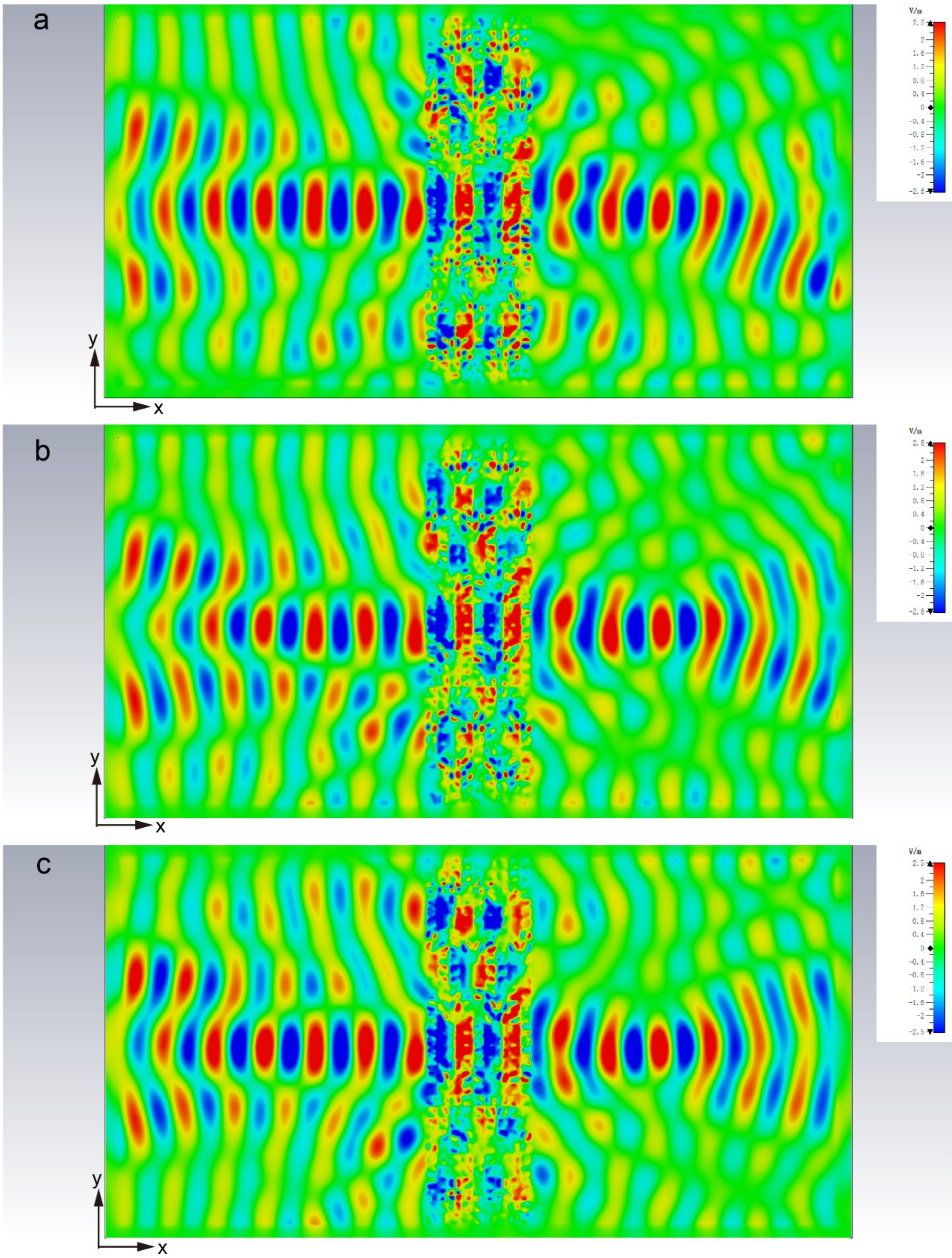

Fig. S6 (a, b, c) Simulated field distributions of Re(E_z) under *x*-pol plane wave incidence on a plane 50 μm above the device composed of meta-atoms with different linear factors of (a) 1.00, (b) 1.18, and (c) 1.39, at 0.24 THz.